First Observation of the $\bar{B}_s^0 \to \Lambda_c^+ \bar{\Lambda}_c^-$ Decay and Evidence for the $\bar{B}^0 \to \Lambda_c^+ \bar{\Lambda}_c^-$ Decay

R. Aaij *et al.*[*]
(LHCb Collaboration)

(Received 30 November 2025; accepted 14 January 2026; published 13 February 2026)

A search is presented for the two-body charmed baryonic decays, $\bar{B}_{(s)}^0 \to \Lambda_c^+ \bar{\Lambda}_c^-$, using a data sample collected by the LHCb experiment during 2011–2012 and 2015–2018, corresponding to an integrated luminosity of 9 fb^{-1}. The first observation of the $\bar{B}_s^0 \to \Lambda_c^+ \bar{\Lambda}_c^-$ decay is reported with 6.2σ significance along with 4.3σ evidence for the $\bar{B}^0 \to \Lambda_c^+ \bar{\Lambda}_c^-$ decay. The branching fractions are measured to be $\mathcal{B}(\bar{B}^0 \to \Lambda_c^+ \bar{\Lambda}_c^-) = (1.01^{+0.27}_{-0.28} \pm 0.08 \pm 0.15) \times 10^{-5}$ and $\mathcal{B}(\bar{B}_s^0 \to \Lambda_c^+ \bar{\Lambda}_c^-) = (5.0 \pm 1.3 \pm 0.5 \pm 0.8) \times 10^{-5}$, where the first uncertainty is statistical, the second systematic, and the third due to external inputs. These results provide novel experimental inputs for the theoretical framework describing two-body baryonic decays of B mesons via W-emission and W-exchange mechanisms.

DOI: 10.1103/cxn3-8t4g

The study of B-meson decays has long been a fertile ground for testing the standard model of particle physics and probing for potential new physics beyond it. Among the diverse decay channels, baryonic decays of B mesons provide a unique laboratory for exploring the interplay between weak interactions and quantum chromodynamics in the nonperturbative regime [1,2]. These decays are not only sensitive to the Cabibbo-Kobayashi-Maskawa matrix elements [3,4], but they also offer insights into the dynamics of baryon production and final-state interactions, which are less understood compared to mesonic systems.

In the standard model, two-body baryonic B-meson decays proceed at tree level through the nonfactorizable internal W-emission quark diagram and the factorizable W-exchange and W-annihilation topology. However, the W-exchange and -annihilation processes can be helicity suppressed [5,6], and hence, are often neglected in theoretical studies [7–13]. Experimental searches for the factorizable topology are currently limited to the $\bar{B}_s^0 \to p\bar{p}$ decay [14], with an upper limit on the branching fraction $\mathcal{B}$ set at 4.4×10^{-9} at 90% confidence level (CL) [15]. However, other theories suggest that processes with quark-level $b \to c$ transitions, such as $\bar{B}_s^0 \to \Lambda_c^+ \bar{\Lambda}_c^-$, $\bar{B}^0 \to \Xi_c^+ \bar{\Xi}_c^-$, and $\bar{B}_s^0 \to p \bar{\Lambda}_c^-$, can circumvent severe helicity suppression, making the factorizable topology nonnegligible [16–18] and potentially leading to sizable direct CP asymmetries [13].

As illustrated in the Feynman diagrams in Fig. 1, the two-body charmed decays $\bar{B}^0 \to \Lambda_c^+ \bar{\Lambda}_c^-$ are expected to proceed mainly through tree-level W-emission amplitudes, while $\bar{B}_s^0 \to \Lambda_c^+ \bar{\Lambda}_c^-$ decays are expected to proceed via suppressed topologies [19]. As a consequence, the $\bar{B}^0 \to \Lambda_c^+ \bar{\Lambda}_c^-$ branching fraction is expected to be larger than that of the corresponding $\bar{B}_s^0$-meson decay. If the $\bar{B}^0 \to \Lambda_c^+ \bar{\Lambda}_c^-$ decay proceeds similarly to $B^- \to \Xi_c^0 \bar{\Lambda}_c^-$ and $\bar{B}^0 \to \Xi_c^+ \bar{\Lambda}_c^-$ decays, which are also believed to be dominated by the nonfactorizable W-emission topology, then its branching fraction is expected to be $|V_{cd}/V_{cs}|^2 (\tau_{B^0}/\tau_{B^+}) \mathcal{B}(B^- \to \Xi_c^0 \bar{\Lambda}_c^-) = (4.7 \pm 1.1) \times 10^{-5}$ in the U-spin symmetry limit. Here, the CKM matrix elements V_{cd} and V_{cs}, along with the B^0 and B^+ meson lifetimes τ_{B^0} and τ_{B^+}, are taken from Ref. [20]. While the Belle Collaboration has reported an upper limit on the $\bar{B}^0 \to \Lambda_c^+ \bar{\Lambda}_c^-$ branching fraction of 6.2×10^{-5} at 90% CL [21], consistent with this prediction, the LHCb Collaboration has determined more strict upper limits of 1.6×10^{-5} and 8.0×10^{-5} at 95% CL for the $\bar{B}^0 \to \Lambda_c^+ \bar{\Lambda}_c^-$ and $\bar{B}_s^0 \to \Lambda_c^+ \bar{\Lambda}_c^-$ branching fractions, respectively [22]. These measured upper limits suggest a tension between theory and experiment, indicating a contribution from W-exchange or interference effects, which requires more precision measurements for confirmation.

This Letter presents a search for $\bar{B}_{(s)}^0 \to \Lambda_c^+ (pK^-\pi^+) \bar{\Lambda}_c^- (\bar{p}K^+\pi^-)$ decays using proton-proton (pp) collision data collected with the LHCb detector at center-of-mass energies of 7, 8, and 13 TeV during the LHC Run 1 (2011–2012) and Run 2 (2015–2018) data-taking periods, corresponding to a total integrated luminosity of 9 fb^{-1}. The branching fractions of the signal decays are measured relative to the topologically similar $\bar{B}^0 \to D_s^- (K^+K^-\pi^-) D^+ (K^-\pi^+\pi^+)$ and $\bar{B}_s^0 \to D_s^+ (K^-K^+\pi^+) D_s^- (K^+K^-\pi^-)$

---

[*] Full author list given at the end of the Letter.

Published by the American Physical Society under the terms of the Creative Commons Attribution 4.0 International license. Further distribution of this work must maintain attribution to the author(s) and the published article's title, journal citation, and DOI. Funded by SCOAP³.

© 2026 CERN, for the LHCb Collaboration

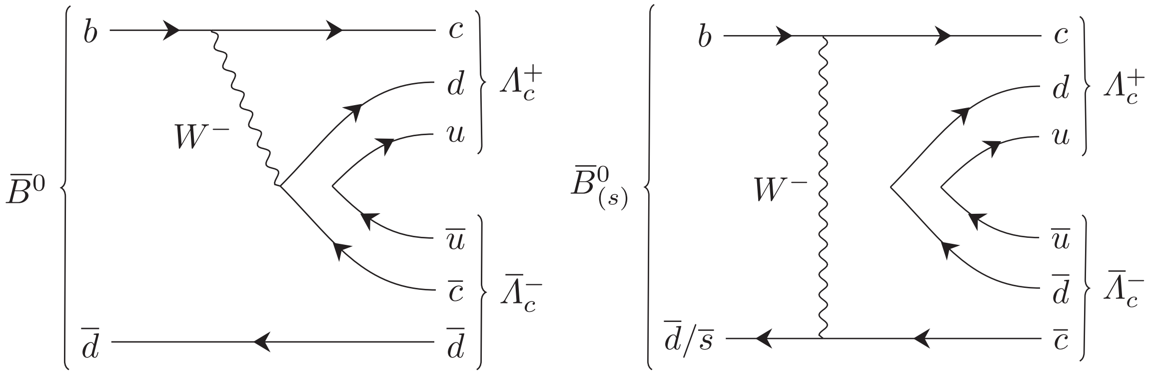

FIG. 1. Tree-level Feynman diagrams for $\bar{B}^0_{(s)} \to \Lambda_c^+ \bar{\Lambda}_c^-$ decays. The left diagram shows the contribution from the W-emission process, while the right one depicts the W-exchange process.

normalization channels using

$$\mathcal{B}(\bar{B}^0 \to \Lambda_c^+ \bar{\Lambda}_c^-) = \mathcal{B}(\bar{B}^0 \to D_s^- D^+) \cdot \frac{\mathcal{B}_{D_s^+}\mathcal{B}_{D^+}}{\mathcal{B}^2_{\Lambda_c^+}} \cdot \frac{N(\bar{B}^0 \to \Lambda_c^+ \bar{\Lambda}_c^-)}{N(\bar{B}^0 \to D_s^- D^+)} \cdot \frac{\epsilon(\bar{B}^0 \to D_s^- D^+)}{\epsilon(\bar{B}^0 \to \Lambda_c^+ \bar{\Lambda}_c^-)},$$

$$\mathcal{B}(\bar{B}^0_s \to \Lambda_c^+ \bar{\Lambda}_c^-) = \mathcal{B}(\bar{B}^0_s \to D_s^+ D_s^-) \cdot \frac{\mathcal{B}^2_{D_s^+}}{\mathcal{B}^2_{\Lambda_c^+}} \cdot \frac{N(\bar{B}^0_s \to \Lambda_c^+ \bar{\Lambda}_c^-)}{N(\bar{B}^0_s \to D_s^+ D_s^-)} \cdot \frac{\epsilon(\bar{B}^0_s \to D_s^+ D_s^-)}{\epsilon(\bar{B}^0_s \to \Lambda_c^+ \bar{\Lambda}_c^-)},$$

where N denotes the measured yield; ϵ represents the combined efficiency, including the detector acceptance, trigger, reconstruction, and selection efficiencies; and $\mathcal{B}_{D_s^+}$, $\mathcal{B}_{D^+}$, and $\mathcal{B}_{\Lambda_c^+}$ denote the known branching fractions of $D_s^+ \to K^- K^+ \pi^+$, $D^+ \to K^- \pi^+ \pi^+$, and $\Lambda_c^+ \to p K^- \pi^+$ decays, respectively [20].

The LHCb detector is a single-arm forward spectrometer covering the pseudorapidity range $2 < \eta < 5$, described in detail in Refs. [23,24]. The online event selection is performed by a trigger [25,26], which consists of a hardware stage followed by a two-level software stage that applies a full event reconstruction. At the hardware trigger stage, events are required to have a hadron, photon, or electron with high transverse energy in the calorimeters. For hadrons, the transverse energy threshold is 3.5 GeV. At the software trigger stage, there must be a secondary vertex consistent with a two-, three-, or four-body decay topology, with significant displacement from any primary pp collision vertex (PV). At least one charged particle must have a transverse momentum $p_{\mathrm{T}} > 1.6$ GeV and be inconsistent with originating from any PV [27].

Simulated samples are used to study the properties of the signal, normalization, and background channels. Proton-proton collisions are generated by PYTHIA [28] with a specific LHCb configuration [29]. Decays of unstable particles are described by EvtGen [30], in which final-state radiation is generated using PHOTOS [31]. The interactions of the generated particles with the detector material, and their responses, are implemented using the Geant4 toolkit [32,33], as described in Ref. [34].

In the offline selection, the candidate decays are reconstructed by first forming Λ_c^+ (or $D^+_{(s)}$) candidates from three-track combinations and then combining pairs of these charmed hadrons into $\bar{B}^0_{(s)}$ mesons. Each final-state particle must fulfill the momentum requirements $p > 5$ GeV, $p_{\mathrm{T}} > 500$ MeV, and must be inconsistent with originating from any PV using the criterion $\chi^2_{\mathrm{IP}} > 4$, where χ^2_{IP} is the difference between the vertex-fit χ^2 of a given PV reconstructed with and without the particle in question. For proton candidates, a more stringent requirement $p > 10$ GeV is imposed. In addition, a loose particle identification (PID) requirement is applied to all charged tracks [35,36]. The charmed hadrons are required to satisfy $p_{\mathrm{T}} > 1$ GeV with a good-quality decay vertex significantly separated from any PV. To further suppress singly charmed and charmless background sources, the measured decay length along the beamline direction for each charmed hadron candidate must be greater than half of its resolution. Subsequently, a good $\bar{B}^0_{(s)}$ decay vertex is required, which must be significantly displaced from the associated PV, defined as the PV for which the particle has the smallest χ^2_{IP}. The momentum of the $\bar{B}^0_{(s)}$ candidate is required to be consistent with its flight direction. To suppress background arising from the misreconstruction of a single charged-particle trajectory as two or more distinct tracks, candidate decays are rejected if the opening angle between the momentum vectors of any pair of final-state tracks is less than 0.5 mrad.

To suppress cross-feed among Λ_c^+, D_s^+, and D^+ candidates, veto criteria are implemented based on invariant-mass and PID requirements. For $\Lambda_c^+ \to pK^-\pi^+$ decays, candidates are rejected if the pK^- invariant mass, after assigning the kaon mass to the proton candidate, lies within ±10 MeV of the known $\phi(1020)$ mass [20]. Additional PID requirements are applied when the reconstructed $pK^-\pi^+$ invariant mass lies within ±25 MeV of the known D^+ (D_s^+) mass after assigning the pion (kaon) mass hypothesis to the proton candidate. Similarly, a tighter PID requirement is applied to the K^+ meson in $D_s^+ \to K^-K^+\pi^+$ decays for events where the invariant mass of the K^- K^+ π^+ combination, computed after assigning the pion (proton) mass to the kaon, falls within ±25 MeV of the D^+ (Λ_c^+) mass. In the case of $D^+ \to K^-\pi^+\pi^+$ decays, after assigning the mass of either of the two pions to the kaon (proton), candidates with $K^-\pi^+\pi^+$ invariant mass within ±25 MeV of the D_s^+ (Λ_c^+) mass are rejected unless a tighter PID requirement is fulfilled.

The two most powerful variables for discriminating between signal and the remaining combinatorial background are the χ^2_{IP} of the $\bar{B}^0_{(s)}$ candidate with respect to its PV and the quantity $\prod_i \mathcal{P}_i$. The latter is defined as the product of the neural-network-based PID variables for correct identification of all six final-state particles [24]. As the PID algorithms are tuned individually for Run 1 and Run 2 operations, the $\prod_i \mathcal{P}_i$ optimization is performed separately for each data-taking period. The selection criteria for these two variables are determined using data from the sideband region, $5150 < m(\Lambda_c^+\bar{\Lambda}_c^-) < 5240$ MeV or $5407 < m(\Lambda_c^+\bar{\Lambda}_c^-) < 5550$ MeV as background proxy, and simulated $\bar{B}^0_s \to \Lambda_c^+\bar{\Lambda}_c^-$ samples as signal proxy, with the goal of maximizing the Punzi figure of merit $\epsilon/[(\sigma/2) + \sqrt{N_{\mathrm{B}}}]$ [37]. Here, ϵ represents the signal efficiency for a given selection criterion, σ denotes the target signal significance (set to 5), and N_{B} corresponds to the background yield in the signal region $5350 < m(\Lambda_c^+\bar{\Lambda}_c^-) < 5380$ MeV. The optimized $\prod_i \mathcal{P}_i$ and χ^2_{IP} selection criteria, determined separately for Run 1 and Run 2, are applied to all data and simulation samples.

To ensure a realistic description of the data, the kinematic distributions and the PID variables of charged tracks in simulated samples are corrected. The kinematic correction accounts for dependencies on p_{T}, η, event multiplicity, and χ^2_{IP} of the $\bar{B}^0_{(s)}$ candidate. The correction weights are determined through a data-driven approach employing a gradient-boosting algorithm [38], where background-subtracted data samples are obtained using the *sPlot* technique [39] applied to normalization decay modes. The PID variables are calibrated via a kinematic-dependent transformation, where a kernel density estimation (KDE) algorithm is used to provide a smooth interpolation of distributions from dedicated calibration samples [36].

Efficiencies are derived from simulated samples after applying the corrections outlined above and imposing all selection criteria. The efficiency ratios between signal and normalization channels are determined separately for each data-taking year, and then averaged according to the integrated luminosity of each sample, giving overall values $\epsilon(\bar{B}^0 \to \Lambda_c^+\bar{\Lambda}_c^-)/\epsilon(\bar{B}^0 \to D_s^- D^+) = 0.67 \pm 0.01$ and $\epsilon(\bar{B}^0_s \to \Lambda_c^+\bar{\Lambda}_c^-)/\epsilon(\bar{B}^0_s \to D_s^+ D_s^-) = 0.56 \pm 0.01$. The uncertainties are purely due to the limited size of the simulation samples.

The $\bar{B}^0_{(s)} \to \Lambda_c^+\bar{\Lambda}_c^-$ yields are obtained from a two-stage fitting procedure. The first stage is an unbinned maximum-likelihood fit to the two-dimensional $[m(\Lambda_c^+), m(\bar{\Lambda}_c^-)]$ distribution, aiming to separate genuine Λ_c^+ $\bar{\Lambda}_c^-$ candidates from charmless and singly charmed backgrounds. This fit is performed in 5 MeV bins of $m(\Lambda_c^+\bar{\Lambda}_c^-)$ to determine background-subtracted yields. In this fit, the Λ_c^+ or $\bar{\Lambda}_c^-$ signal is described by a modified crystal ball distribution [40] with tails on both sides of the Gaussian core (double-sided crystal ball, DSCB), where the tail parameters are fixed to those found in simulation, and the peak position is allowed to vary among different $m(\Lambda_c^+\bar{\Lambda}_c^-)$ bins to account for possible correlations between the $\bar{B}^0_{(s)}$ mass and the Λ_c^+ ($\bar{\Lambda}_c^-$) mass. In the baseline fit, the ratio of widths of the Λ_c^+ peak between data and simulation is constrained with Gaussian priors to the value derived from the normalization channel. The background in each dimension is described by an exponential function. The construction of the fit model and the corresponding results are detailed in the End Matter.

The second stage is a binned maximum-likelihood fit to the resulting $m(\Lambda_c^+\bar{\Lambda}_c^-)$ distribution of the doubly charmed decays, as shown in Fig. 2, to determine the $\bar{B}^0 \to \Lambda_c^+\bar{\Lambda}_c^-$ and $\bar{B}^0_s \to \Lambda_c^+\bar{\Lambda}_c^-$ signal yields, with potential background from nonpeaking Λ_c^+ $\bar{\Lambda}_c^-$ also included. The $\bar{B}^0_{(s)}$ signal

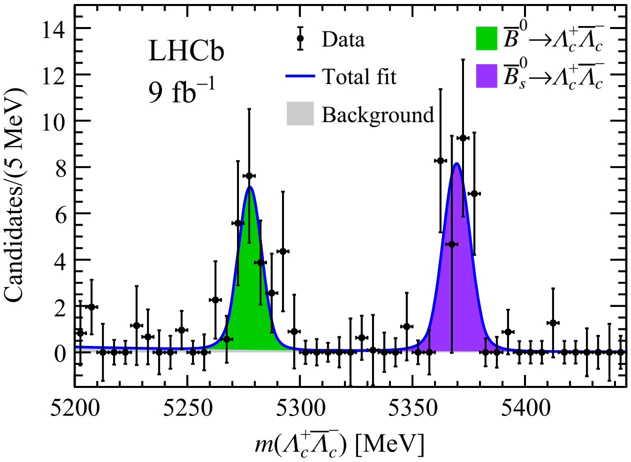

FIG. 2. Mass distribution of the $\Lambda_c^+\bar{\Lambda}_c^-$ system with singly charmed and charmless backgrounds subtracted. The fit result (blue curve) is shown together with the signal components from $\bar{B}^0 \to \Lambda_c^+\bar{\Lambda}_c^-$ (filled green) and $\bar{B}^0_s \to \Lambda_c^+\bar{\Lambda}_c^-$ (filled purple) decays and the nonresonant background contribution (filled gray).

shape is described by a DSCB distribution with the tail parameters fixed from simulation. Widths of the $\bar{B}^0$ and $\bar{B}^0_s$ peaks are fixed to the values measured for the corresponding normalization channels scaled by the ratio of signal to normalization widths determined from simulation. The background shape is assumed to be exponential, with the slope parameter free to vary in the fit. The $\bar{B}^0 \to \Lambda_c^+ \bar{\Lambda}_c^-$ and $\bar{B}^0_s \to \Lambda_c^+ \bar{\Lambda}_c^-$ signal yields obtained from the fit to the samples are $19.0^{+5.0}_{-5.2}$ and 25.1 ± 6.7, respectively, where the uncertainties are statistical only and determined from pseudoexperiments.

The normalization channel yields are obtained using a similar two-stage fitting procedure as for the signal channels, where the $\bar{B}^0_{(s)}$ and $D^+_{(s)}$ signal and background components are modeled using the same line shapes as the $\bar{B}^0_{(s)} \to \Lambda_c^+ \bar{\Lambda}_c^-$ decays. The line shape for the misidentified $\bar{B}^0 \to D_s^- D^+$ decay in the $\bar{B}^0_s \to D_s^+ D_s^-$ dataset is estimated from simulated samples using the KDE approach [41]. The fits yield 26171 ± 164 $\bar{B}^0 \to D_s^- D^+$ signal decays and 2926 ± 65 $\bar{B}^0_s \to D_s^+ D_s^-$ signal decays, with the fit projections provided in the End Matter.

Several sources of systematic uncertainty from the mass fit and the efficiency ratio are considered. A summary is presented in Table I. Alternative mass fits are performed with different configurations of the fit model, and the largest change in the branching ratio is assigned as the corresponding systematic uncertainty. The signal models are varied to use either fixed or Gaussian-constrained widths for the $B^0_{(s)}$ peaks and either Gaussian-constrained or floated widths for the Λ_c^+ peak. Alternative signal models for Λ_c^+, $D^+_{(s)}$, and $B^0_{(s)}$ peaks are tested either by varying the DSCB tail parameters or by replacing the DSCB distribution with a Hypatia [42] distribution. The exponential background shapes are replaced with Chebyshev polynomials. The line shape of the misidentified $\bar{B}^0 \to D_s^- D^+$ decay in the $\bar{B}^0_s \to D_s^+ D_s^-$ dataset is replaced by an alternative KDE with a 50% wider sampling width. The fitting procedure is validated using pseudoexperiments. A bias at a level of a few percent is observed in the fitted signal yield, mainly arising from the positivity constraint on the signal yields in the first-stage fit and the inherent bias of maximum-likelihood fits with small yields [43]. The size of this bias is assigned as a systematic uncertainty.

Systematic uncertainties associated with the efficiencies estimated from simulation are also evaluated. Limited knowledge of the detector material budget and particle interaction cross sections leads to uncertainties on the tracking efficiencies, which are estimated using the approaches provided in Ref. [44]. The corrections applied to the PID variables in the simulation depend on both the sample size of the calibration datasets and the kernel densities used in the sampling. To evaluate the systematic uncertainty, the KDE template is varied by increasing the kernel width by 50% and by implementing a bootstrapping technique. The uncertainties arising from the limited size of the simulated samples are estimated under the assumption that the efficiencies follow binomial distributions. A systematic uncertainty associated with the kinematical correction procedure is evaluated by performing an alternative correction that employs a different set of kinematic variables to train the weighting algorithm. The systematic uncertainty associated with imperfect simulation of the hardware trigger is estimated using a data-driven method [25,26] and found to be negligible. This is expected, given the similar kinematics and decay topologies between the signal and normalization decays.

To address uncertainties due to the treatment in simulation of intermediate states in the $\Lambda_c^+ \to p K^- \pi^+$ decay and

TABLE I. Relative systematic uncertainties on the measured branching fraction ratios. The dashes indicate sources that are not relevant for that measurement.

Source	$[\mathcal{B}(\bar{B}^0 \to \Lambda_c^+ \bar{\Lambda}_c^-)/\mathcal{B}(\bar{B}^0 \to D_s^- D^+)]$ (%)	$[\mathcal{B}(\bar{B}^0_s \to \Lambda_c^+ \bar{\Lambda}_c^-)/\mathcal{B}(\bar{B}^0_s \to D_s^+ D_s^-)]$ (%)
Λ_c^+ peak width	2.1	4.3
$\bar{B}^0_{(s)}$ peak width	0.2	0.5
Λ_c^+ or $D^+_{(s)}$ line shape	0.2	0.2
$\bar{B}^0_{(s)}$ signal line shape	3.6	0.5
Background line shape	1.4	7.1
Line shape of misidentified decay	not applicable	0.1
Fit bias	5.7	1.2
Tracking efficiency	1.3	1.6
PID correction	0.7	0.9
Simulated sample size	1.7	1.8
Kinematical correction	0.2	0.3
Λ_c^+ Dalitz plot and polarization correction	3.6	4.3
$\bar{B}^0_s$ lifetime correction	not applicable	0.6
Total	8.4	9.9

the Λ_c^+ -baryon polarization, two weighting procedures are implemented. The Λ_c^+ Dalitz plot distributions in simulation are weighted to match those in data. Then, the Λ_c^+ polarization is emulated by a weight $1 + \alpha P \cos\theta_p$, where θ_p is the angle between the proton momentum in the Λ_c^+ rest frame and the Λ_c^+ direction in the $\bar{B}^0_{(s)}$ rest frame. The decay parameter α and polarization P are taken from Ref. [45]. The systematic uncertainty is evaluated as the relative difference between results with and without these weights applied. An additional systematic uncertainty is assigned to account for the difference between the average $\bar{B}^0_s$ lifetime used in simulation and the physical lifetimes of the decay modes, which are dominated by the shorter-lived $\bar{B}^0_s$ mass eigenstate for both signal and normalization modes. The effect is evaluated by reweighting the $\bar{B}^0_s$ lifetime distribution in simulated samples and found to be small.

After evaluating the systematic uncertainties, the branching fractions are measured as

$$\mathcal{B}(\bar{B}^0 \to \Lambda_c^+\bar{\Lambda}_c^-) = (1.01^{+0.27}_{-0.28} \pm 0.08 \pm 0.15) \times 10^{-5},$$
$$\mathcal{B}(\bar{B}^0_s \to \Lambda_c^+\bar{\Lambda}_c^-) = (5.0 \pm 1.3 \pm 0.5 \pm 0.8) \times 10^{-5},$$

where the uncertainties, respectively, represent statistical, systematic, and external contributions from branching fractions of intermediate charmed decays and normalization channels [20].

To evaluate the significance of each signal decay, a test statistic $q = -2\ln(\mathcal{L}_0/\hat{\mathcal{L}})$ is defined, where $\mathcal{L}_0$ represents the likelihood of the model with the contribution from either $\bar{B}^0 \to \Lambda_c^+\bar{\Lambda}_c^-$ or $\bar{B}^0_s \to \Lambda_c^+\bar{\Lambda}_c^-$ removed, and $\hat{\mathcal{L}}$ corresponds to the likelihood when both contributions are included. Among all the fit variants discussed above, the model yielding the minimal q value in the data is identified. Datasets from pseudoexperiments are then generated by excluding either $\bar{B}^0$ or $\bar{B}^0_s$ contributions from this model. The p values associated with the observed $\bar{B}^0$ and $\bar{B}^0_s$ signals in the data are calculated from the tails of the two resulting q distributions derived from these datasets and then converted to significances. The resulting significance, considering the systematic uncertainty, is 4.3σ for the $\bar{B}^0 \to \Lambda_c^+\bar{\Lambda}_c^-$ decay and 6.2σ for the $\bar{B}^0_s \to \Lambda_c^+\bar{\Lambda}_c^-$ decay.

In summary, we present the first measurements of $\bar{B}^0 \to \Lambda_c^+\bar{\Lambda}_c^-$ and $\bar{B}^0_s \to \Lambda_c^+\bar{\Lambda}_c^-$ branching fractions using the complete LHCb Run 1 and Run 2 datasets. The first observation of the $\bar{B}^0_s \to \Lambda_c^+\bar{\Lambda}_c^-$ decay represents the first experimental verification of the W-exchange process in baryonic B-meson decays, a mechanism long considered helicity suppressed, and therefore, often neglected. The measured value of $\mathcal{B}(\bar{B}^0 \to \Lambda_c^+\bar{\Lambda}_c^-)$ is at the level of 1×10^{-5}, indicating a significant discrepancy with the expected contribution from the W-emission diagram alone, as presented earlier in this Letter. This deviation provides further evidence for the presence of SU(3)-breaking effects and a W-exchange contribution that interferes destructively with the internal W-emission process, thereby suppressing the observed branching fraction. Taken together, these observations suggest that the long-overlooked contribution from W-annihilation and -exchange mechanisms in charmless, singly charmed, and doubly charmed two-body baryonic B-meson decays needs a thorough reexamination. Such effects may be important for improving predictions of CP -violating phenomena in baryonic B decays, which could potentially be studied using data from LHCb Run 3 and future upgrades [46,47].

Acknowledgments—We express our gratitude to our colleagues in the CERN accelerator departments for the excellent performance of the LHC. We thank the technical and administrative staff at the LHCb institutes. We acknowledge support from CERN and from the national agencies: ARC (Australia); CAPES, CNPq, FAPERJ, and FINEP (Brazil); MOST and NSFC (China); CNRS/IN2P3 (France); BMFTR, DFG, and MPG (Germany); INFN (Italy); NWO (Netherlands); MNiSW and NCN (Poland); MCID/IFA (Romania); MICIU and AEI (Spain); SNSF and SER (Switzerland); NASU (Ukraine); STFC (United Kingdom); DOE NP and NSF (USA). We acknowledge the computing resources that are provided by ARDC (Australia), CBPF (Brazil), CERN, IHEP and LZU (China), IN2P3 (France), KIT and DESY (Germany), INFN (Italy), SURF (Netherlands), Polish WLCG (Poland), IFIN-HH (Romania), PIC (Spain), CSCS (Switzerland), and GridPP (United Kingdom). We are indebted to the communities behind the multiple open-source software packages on which we depend. Individual groups or members have received support from Key Research Program of Frontier Sciences of CAS, CAS PIFI, CAS CCEPP, Minciencias (Colombia); EPLANET, Marie Skłodowska-Curie Actions, ERC, and NextGenerationEU (European Union); A*MIDEX, ANR, IPhU and Labex P2IO, and Rêgion Auvergne-Rhône-Alpes (France); Alexander-von-Humboldt Foundation (Germany); ICSC (Italy); Severo Ochoa and María de Maeztu Units of Excellence, GVA, XuntaGal, GENCAT, InTalent-Inditex, and Prog. Atracción Talento CM (Spain); SRC (Sweden); the Leverhulme Trust, the Royal Society, and UKRI (United Kingdom).

Data availability—The data that support the findings of this article are openly available [48].

[1] H.-Y. Cheng, Status of baryonic B decays, Nucl. Phys. B, Proc. Suppl. **163**, 68 (2007).

[2] X. Huang, Y.-K. Hsiao, J. Wang, and L. Sun, Baryonic B meson decays, Adv. High Energy Phys. **2022**, 4343824 (2022).

[3] N. Cabibbo, Unitary symmetry and leptonic decays, Phys. Rev. Lett. **10**, 531 (1963).

[4] M. Kobayashi and T. Maskawa, *CP*-violation in the renormalizable theory of weak interaction, Prog. Theor. Phys. **49**, 652 (1973).

[5] C.-H. Chen, H.-Y. Cheng, and Y.-K. Hsiao, Baryonic D decay $D_s^+ \to p\bar{n}$ and its implication, Phys. Lett. B **663**, 326 (2008).

[6] A. J. Bevan *et al.* (*BABAR* and Belle Collaborations), The physics of the B factories, Eur. Phys. J. C **74**, 3026 (2014).

[7] V. L. Chernyak and I. R. Zhitnitsky, B-meson exclusive decays into baryons, Nucl. Phys. **B345**, 137 (1990).

[8] H.-Y. Cheng and K.-C. Yang, Charmless exclusive baryonic B decays, Phys. Rev. D **66**, 014020 (2002).

[9] C.-H. V. Chang and W.-S. Hou, B meson decays to baryons in the diquark model, Eur. Phys. J. C **23**, 691 (2002).

[10] C.-K. Chua, Charmless two-body baryonic $B_{u,d,s}$ decays revisited, Phys. Rev. D **89**, 056003 (2014).

[11] X.-G. He, T. Li, X.-Q. Li, and Y.-M. Wang, Calculation of $\mathcal{B}(\bar{B}^0 \to \Lambda_c^+ + \bar{p})$ in the perturbative QCD approach, Phys. Rev. D **75**, 034011 (2007).

[12] H.-Y. Cheng, C.-K. Chua, and Y.-K. Hsiao, Study of $\bar{B} \to \Lambda_c\bar{\Lambda}_c$ and $\bar{B} \to \Lambda_c\bar{\Lambda}_c\bar{K}$, Phys. Rev. D **79**, 114004 (2009).

[13] C.-Q. Geng, X.-N. Jin, and C.-W. Liu, Large *CP* asymmetries from final-state interactions in charmful baryonic decays of $B^0 \to \Xi_c^+\Xi_c^-$ and $B_s^0 \to \Lambda_c^+\Lambda_c^-$, Phys. Rev. D **112**, 013001 (2025).

[14] Charge-conjugate decays are implied throughout.

[15] R. Aaij *et al.* (LHCb Collaboration), Search for the rare hadronic decay $B_s^0 \to p\bar{p}$, Phys. Rev. D **108**, 012007 (2023).

[16] Y.-K. Hsiao, S.-Y. Tsai, C.-C. Lih, and E. Rodrigues, Testing the W-exchange mechanism with two-body baryonic B decays, J. High Energy Phys. 04 (2020) 035.

[17] Y.-K. Hsiao, Study of two-body doubly charmful baryonic B decays with $SU(3)$ flavor symmetry, J. High Energy Phys. 11 (2023) 117.

[18] C.-Q. Geng, X.-N. Jin, C.-W. Liu, and X. Yu, Hidden strangeness in meson weak decays to baryon pair, Phys. Rev. D **110**, 113008 (2024).

[19] Z. Rui, Z.-T. Zou, and Y. Li, Higher twist corrections to doubly-charmed baryonic B decays, J. High Energy Phys. 12 (2024) 159.

[20] S. Navas *et al.* (Particle Data Group), Review of particle physics, Phys. Rev. D **110**, 030001 (2024).

[21] Y. Uchida *et al.* (Belle Collaboration), Search for $\bar{B}^0 \to \Lambda_c^+\bar{\Lambda}_c^-$ decay at Belle, Phys. Rev. D **77**, 051101 (2008).

[22] R. Aaij *et al.* (LHCb Collaboration), Study of beauty hadron decays into pairs of charm hadrons, Phys. Rev. Lett. **112**, 202001 (2014).

[23] A. A. Alves, Jr. *et al.* (LHCb Collaboration), The LHCb detector at the LHC, J. Instrum. **3**, S08005 (2008).

[24] R. Aaij *et al.* (LHCb Collaboration), LHCb detector performance, Int. J. Mod. Phys. A **30**, 1530022 (2015).

[25] R. Aaij *et al.*, The LHCb trigger and its performance in 2011, J. Instrum. **8**, P04022 (2013).

[26] R. Aaij *et al.*, Design and performance of the LHCb trigger and full real-time reconstruction in Run 2 of the LHC, J. Instrum. **14**, P04013 (2019).

[27] Natural units with $\hbar = c = 1$ are used throughout this Letter.

[28] T. Sjöstrand, S. Mrenna, and P. Skands, A brief introduction to PYTHIA 8.1, Comput. Phys. Commun. **178**, 852 (2008).

[29] I. Belyaev *et al.*, Handling of the generation of primary events in Gauss, the LHCb simulation framework, J. Phys. Conf. Ser. **331**, 032047 (2011).

[30] D. J. Lange, The EvtGen particle decay simulation package, Nucl. Instrum. Methods Phys. Res., Sect. A **462**, 152 (2001).

[31] N. Davidson, T. Przedzinski, and Z. Was, PHOTOS interface in C++: Technical and physics documentation, Comput. Phys. Commun. **199**, 86 (2016).

[32] S. Agostinelli *et al.* (Geant4 Collaboration), Geant4: A simulation toolkit, Nucl. Instrum. Methods Phys. Res., Sect. A **506**, 250 (2003).

[33] J. Allison *et al.* (Geant4 Collaboration), Geant4 developments and applications, IEEE Trans. Nucl. Sci. **53**, 270 (2006).

[34] M. Clemencic, G. Corti, S. Easo, C. R. Jones, S. Miglioranzi, M. Pappagallo, and P. Robbe, The LHCb simulation application, Gauss: Design, evolution and experience, J. Phys. Conf. Ser. **331**, 032023 (2011).

[35] M. Adinolfi *et al.*, Performance of the LHCb RICH detector at the LHC, Eur. Phys. J. C **73**, 2431 (2013).

[36] L. Anderlini *et al.*, The PIDCalib package, LHCb-PUB-2016-021, 2016, https://cds.cern.ch/record/2202412.

[37] G. Punzi, Sensitivity of searches for new signals and its optimization, eConf C **030908**, MODT002 (2003) [arXiv:physics/0308063].

[38] A. Rogozhnikov, Reweighting with boosted decision trees, J. Phys. Conf. Ser. **762**, 012036 (2016).

[39] M. Pivk and F. R. Le Diberder, sPlot: A statistical tool to unfold data distributions, Nucl. Instrum. Methods Phys. Res., Sect. A **555**, 356 (2005).

[40] T. Skwarnicki, A study of the radiative cascade transitions between the Upsilon-prime and Upsilon resonances, Ph.D. thesis, Institute of Nuclear Physics, Krakow, 1986, DESY-F31-86-02.

[41] K. S. Cranmer, Kernel estimation in high-energy physics, Comput. Phys. Commun. **136**, 198 (2001).

[42] D. Martínez Santos and F. Dupertuis, Mass distributions marginalized over per-event errors, Nucl. Instrum. Methods Phys. Res., Sect. A **764**, 150 (2014).

[43] J. A. Rice, *Mathematical Statistics and Data Analysis*, 3rd ed. (Duxbury Press, Belmont, CA, 2006).

[44] LHCb Collaboration, Measurement of the track reconstruction efficiency at LHCb, J. Instrum. **10**, P02007 (2015).

[45] R. Aaij *et al.* (LHCb Collaboration), Amplitude analysis of the $\Lambda_c^+ \to pK^-\pi^+$ decay and Λ_c^+ baryon polarization measurement in semileptonic beauty hadron decays, Phys. Rev. D **108**, 012023 (2023).

[46] LHCb Collaboration, Framework TDR for the LHCb upgrade: Technical design report, Report No. CERN-LHCC-2012-007, 2012.

[47] R. Aaij *et al.* (LHCb Collaboration), The LHCb upgrade I, J. Instrum. **19**, P05065 (2024).

[48] https://cds.cern.ch/record/2949754.

End Matter

Fit to the Λ_c^+–$\bar{\Lambda}_c^-$ mass distribution—A two-dimensional fit model is constructed to describe the $[m(\Lambda_c^+), m(\bar{\Lambda}_c^-)]$ distribution. In each dimension, the peaking component is modeled with a DSCB function $\mathcal{S}$, while the nonresonant background is described by an exponential function $\mathcal{B}$. The total probability density function is constructed from the product of all combinations of $\mathcal{S}$ and $\mathcal{B}$, as

$$\mathcal{P}[m(\Lambda_c^+), m(\bar{\Lambda}_c^-)] = N_{\mathrm{DC}} \cdot [\mathcal{S}(m(\Lambda_c^+))\mathcal{S}(m(\bar{\Lambda}_c^-))] + N_{\mathrm{SC}} \cdot \left[\frac{1}{2}\mathcal{S}(m(\Lambda_c^+))\mathcal{B}(m(\bar{\Lambda}_c^-)) + \frac{1}{2}\mathcal{B}(m(\Lambda_c^+))\mathcal{S}(m(\bar{\Lambda}_c^-))\right] + N_{\mathrm{bkg}} \cdot [\mathcal{B}(m(\Lambda_c^+))\mathcal{B}(m(\bar{\Lambda}_c^-))],$$

where N_{DC}, N_{SC}, and N_{bkg} represent the yields of doubly charmed, singly charmed, and charmless background candidates, respectively. The factor 1/2 arises from the charged-conjugate relationship between the $X \to \Lambda_c^+ \bar{p} K^+ \pi^-$ and $\bar{X} \to \bar{\Lambda}_c^- p K^- \pi^+$ systems and has been verified using simulated samples. The fit is performed individually for each $m(\Lambda_c^+ \bar{\Lambda}_c^-)$ bin, and the corresponding N_{DC} value and its uncertainty are determined. Figure 3 shows the Λ_c^+ and $\bar{\Lambda}_c^-$ mass distributions with the fit results also included, where results from all individual $m(\Lambda_c^+ \bar{\Lambda}_c^-)$ bins are combined to improve visibility.

Fit to the normalization decay modes—Figures 4 and 5 show the $m(D_s^- D^+)$ and $m(D_s^+ D_s^-)$ distributions for the normalization decay modes, respectively, along with the fit projections.

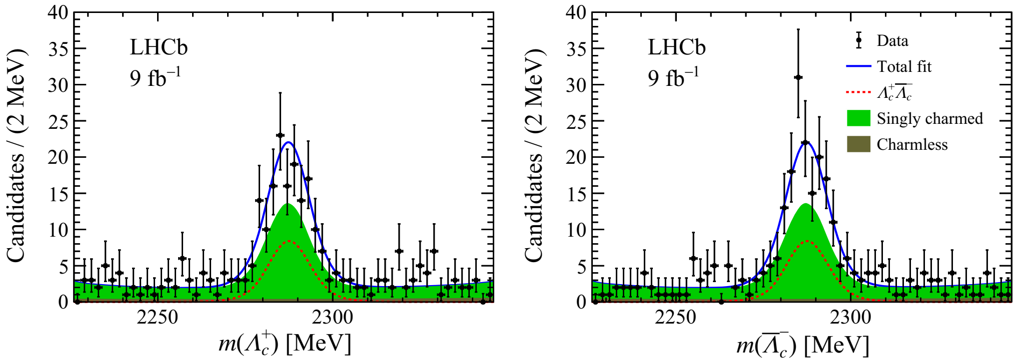

FIG. 3. Distributions of the (left) Λ_c^+ and (right) $\bar{\Lambda}_c^-$ mass for the signal sample. Also shown is the projection of the two-dimensional fit (solid blue line) integrated over all $m(\Lambda_c^+ \bar{\Lambda}_c^-)$ bins, along with the contributions from doubly charmed (dashed red), singly charmed (filled green), and charmless (filled brown) decays.

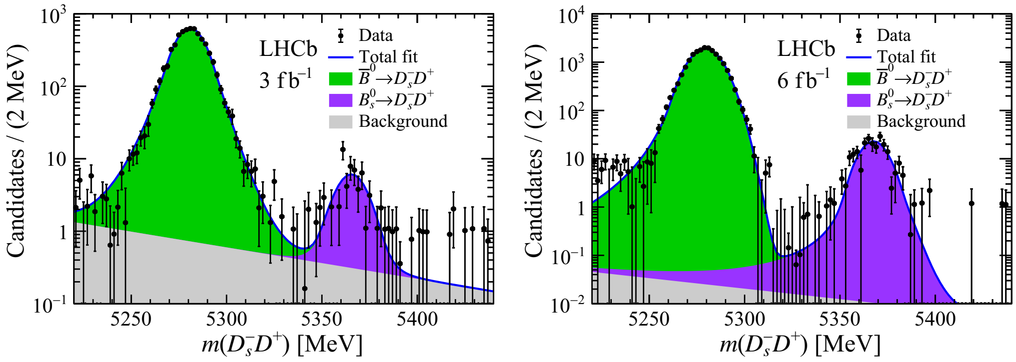

FIG. 4. Mass distribution of the $D_s^- D^+$ system, with singly charmed and charmless backgrounds subtracted, shown for (left) Run 1 and (right) Run 2 data-taking periods. The fit projection (solid blue line) is shown together with the signal components from $\bar{B}^0 \to D_s^- D^+$ (filled green) and $B_s^0 \to D_s^- D^+$ (filled purple) decays and the background contribution (filled gray).

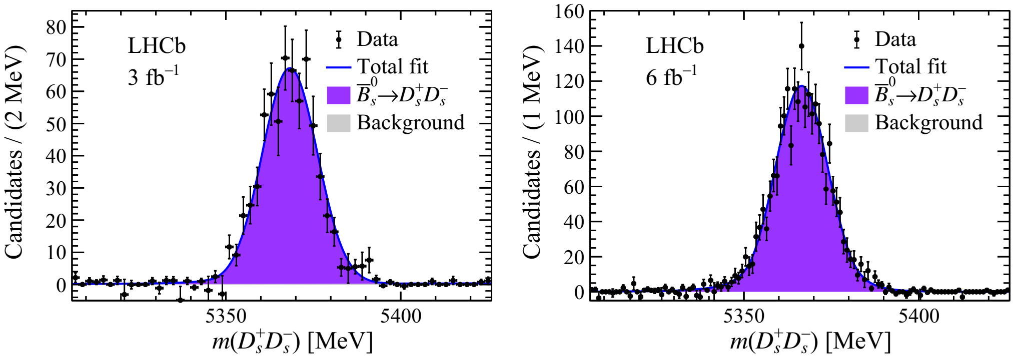

FIG. 5. Mass distribution of the $D_s^+ D_s^-$ system, with singly charmed and charmless backgrounds subtracted, shown for (left) Run 1 and (right) Run 2 data-taking periods. The fit projection (solid blue line) is shown together with the $\bar{B}_s^0 \to D_s^+ D_s^-$ signal (filled purple) and the background (filled gray).

R. Aaij,[38] A. S. W. Abdelmotteleb,[58] C. Abellan Beteta,[52] F. Abudinén,[58] T. Ackernley,[62] A. A. Adefisoye,[70] B. Adeva,[48] M. Adinolfi,[56] P. Adlarson,[86] C. Agapopoulou,[14] C. A. Aidala,[88] Z. Ajaltouni,[11] S. Akar,[11] K. Akiba,[38] M. Akthar,[40] P. Albicocco,[28] J. Albrecht,[19,a] R. Aleksiejunas,[82] F. Alessio,[50] P. Alvarez Cartelle,[57,48] R. Amalric,[16] S. Amato,[3] J. L. Amey,[56] Y. Amhis,[14] L. An,[6] L. Anderlini,[27] M. Andersson,[52] P. Andreola,[52] M. Andreotti,[26] S. Andres Estrada,[45] A. Anelli,[31,b] D. Ao,[7] C. Arata,[12] F. Archilli,[37] Z. Areg,[70] M. Argenton,[26] S. Arguedas Cuendis,[9,50] L. Arnone,[31,b] A. Artamonov,[44] M. Artuso,[70] E. Aslanides,[13] R. Ataíde Da Silva,[51] M. Atzeni,[66] B. Audurier,[12] J. A. Authier,[15] D. Bacher,[65] I. Bachiller Perea,[51] S. Bachmann,[22] M. Bachmayer,[51] J. J. Back,[58] P. Baladron Rodriguez,[48] V. Balagura,[15] A. Balboni,[26] W. Baldini,[26] Z. Baldwin,[80] L. Balzani,[19] H. Bao,[7] J. Baptista de Souza Leite,[2] C. Barbero Pretel,[48,12] M. Barbetti,[27] I. R. Barbosa,[71] R. J. Barlow,[64] M. Barnyakov,[25] S. Barsuk,[14] W. Barter,[60] J. Bartz,[70] S. Bashir,[40] B. Batsukh,[5] P. B. Battista,[14] A. Bavarchee,[81] A. Bay,[51] A. Beck,[66] M. Becker,[19] F. Bedeschi,[35] I. B. Bediaga,[2] N. A. Behling,[19] S. Belin,[48] A. Bellavista,[25] K. Belous,[44] I. Belov,[29] I. Belyaev,[36] G. Benane,[13] G. Bencivenni,[28] E. Ben-Haim,[16] A. Berezhnoy,[44] R. Bernet,[52] S. Bernet Andres,[47] A. Bertolin,[33] F. Betti,[60] J. Bex,[57] O. Bezshyyko,[87] S. Bhattacharya,[81] M. S. Bieker,[18] N. V. Biesuz,[26] A. Biolchini,[38] M. Birch,[63] F. C. R. Bishop,[10] A. Bitadze,[64] A. Bizzeti,[27,c] T. Blake,[58,d] F. Blanc,[51] J. E. Blank,[19] S. Blusk,[70] V. Bocharnikov,[44] J. A. Boelhauve,[19] O. Boente Garcia,[50] T. Boettcher,[69] A. Bohare,[60] A. Boldyrev,[44] C. Bolognani,[84] R. Bolzonella,[26,e] R. B. Bonacci,[1] N. Bondar,[44,50] A. Bordelius,[50] F. Borgato,[33,50] S. Borghi,[64] M. Borsato,[31,b] J. T. Borsuk,[85] E. Bottalico,[62] S. A. Bouchiba,[51] M. Bovill,[65] T. J. V. Bowcock,[62] A. Boyer,[50] C. Bozzi,[26] J. D. Brandenburg,[89] A. Brea Rodriguez,[51] N. Breer,[19] J. Brodzicka,[41] J. Brown,[62] D. Brundu,[32] E. Buchanan,[60] M. Burgos Marcos,[84] A. T. Burke,[64] C. Burr,[50] C. Buti,[27] J. S. Butter,[57] J. Buytaert,[50] W. Byczynski,[50] S. Cadeddu,[32] H. Cai,[76] Y. Cai,[5] A. Caillet,[16] R. Calabrese,[26,e] S. Calderon Ramirez,[9] L. Calefice,[46] M. Calvi,[31,b] M. Calvo Gomez,[47] P. Camargo Magalhaes,[2,f] J. I. Cambon Bouzas,[48] P. Campana,[28] A. C. Campos,[3] A. F. Campoverde Quezada,[7] S. Capelli,[31] M. Caporale,[25] L. Capriotti,[26] R. Caravaca-Mora,[9] A. Carbone,[25,g] L. Carcedo Salgado,[48] R. Cardinale,[29,h] A. Cardini,[32] P. Carniti,[31] L. Carus,[22] A. Casais Vidal,[66] R. Caspary,[22] G. Casse,[62] M. Cattaneo,[50] G. Cavallero,[26] V. Cavallini,[26,e] S. Celani,[50] I. Celestino,[35,i] S. Cesare,[30,j] A. J. Chadwick,[62] I. Chahrour,[88] H. Chang,[4,k] M. Charles,[16] Ph. Charpentier,[50] E. Chatzianagnostou,[38] R. Cheaib,[81] M. Chefdeville,[10] C. Chen,[57] J. Chen,[51] S. Chen,[5] Z. Chen,[7] A. Chen Hu,[63] M. Cherif,[12] A. Chernov,[41] S. Chernyshenko,[54] X. Chiotopoulos,[84] V. Chobanova,[45] M. Chrzaszcz,[41] A. Chubykin,[44] V. Chulikov,[28,36,50] P. Ciambrone,[28] X. Cid Vidal,[48] G. Ciezarek,[50] P. Cifra,[38] P. E. L. Clarke,[60] M. Clemencic,[50] H. V. Cliff,[57] J. Closier,[50] C. Cocha Toapaxi,[22] V. Coco,[50] J. Cogan,[13] E. Cogneras,[11] L. Cojocariu,[43] S. Collaviti,[51]

P. Collins,[50] T. Colombo,[50] M. Colonna,[19] A. Comerma-Montells,[46] L. Congedo,[24] J. Connaughton,[58]
A. Contu,[32] N. Cooke,[61] G. Cordova,[35,i] C. Coronel,[67] I. Corredoira,[12] A. Correia,[16] G. Corti,[50]
J. Cottee Meldrum,[56] B. Couturier,[50] D. C. Craik,[52] M. Cruz Torres,[2,l] M. Cubero Campos,[9] E. Curras Rivera,[51]
R. Currie,[60] C. L. Da Silva,[69] S. Dadabaev,[44] L. Dai,[73] X. Dai,[4] E. Dall'Occo,[50] J. Dalseno,[45]
C. D'Ambrosio,[63] J. Daniel,[11] G. Darze,[3] A. Davidson,[58] J. E. Davies,[64] O. De Aguiar Francisco,[64]
C. De Angelis,[32,m] F. De Benedetti,[50] J. de Boer,[38] K. De Bruyn,[83] S. De Capua,[64] M. De Cian,[64,50]
U. De Freitas Carneiro Da Graca,[2,n] E. De Lucia,[28] J. M. De Miranda,[2] L. De Paula,[3] M. De Serio,[24,o]
P. De Simone,[28] F. De Vellis,[19] J. A. de Vries,[84] F. Debernardis,[24] D. Decamp,[10] S. Dekkers,[1] L. Del Buono,[16]
B. Delaney,[66] J. Deng,[8] V. Denysenko,[52] O. Deschamps,[11] F. Dettori,[32,m] B. Dey,[81] P. Di Nezza,[28]
I. Diachkov,[44] S. Didenko,[44] S. Ding,[70] Y. Ding,[51] L. Dittmann,[22] V. Dobishuk,[54] A. D. Docheva,[61]
A. Doheny,[58] C. Dong,[4,k] A. M. Donohoe,[23] F. Dordei,[32] A. C. dos Reis,[2] A. D. Dowling,[70] L. Dreyfus,[13]
W. Duan,[74] P. Duda,[85] L. Dufour,[50] V. Duk,[34] P. Durante,[50] M. M. Duras,[85] J. M. Durham,[69] O. D. Durmus,[81]
A. Dziurda,[41] A. Dzyuba,[44] S. Easo,[59] E. Eckstein,[18] U. Egede,[1] A. Egorychev,[44] V. Egorychev,[44]
S. Eisenhardt,[60] E. Ejopu,[62] L. Eklund,[86] M. Elashri,[67] D. Elizondo Blanco,[9] J. Ellbracht,[19] S. Ely,[63] A. Ene,[43]
J. Eschle,[70] T. Evans,[38] F. Fabiano,[32] S. Faghih,[67] L. N. Falcao,[31,b] B. Fang,[7] R. Fantechi,[35] L. Fantini,[34,p]
M. Faria,[51] K. Farmer,[60] F. Fassin,[83,38] D. Fazzini,[31,b] L. Felkowski,[85] M. Feng,[5,7] A. Fernandez Casani,[49]
M. Fernandez Gomez,[48] A. D. Fernez,[68] F. Ferrari,[25,g] F. Ferreira Rodrigues,[3] M. Ferrillo,[52] M. Ferro-Luzzi,[50]
S. Filippov,[44] R. A. Fini,[24] M. Fiorini,[26,e] M. Firlej,[40] K. L. Fischer,[65] D. S. Fitzgerald,[88] C. Fitzpatrick,[64]
T. Fiutowski,[40] F. Fleuret,[15] A. Fomin,[53] M. Fontana,[25,50] L. A. Foreman,[64] R. Forty,[50] D. Foulds-Holt,[60]
V. Franco Lima,[3] M. Franco Sevilla,[68] M. Frank,[50] E. Franzoso,[26,e] G. Frau,[64] C. Frei,[50] D. A. Friday,[64,50]
J. Fu,[7] Q. Führing,[19,57,a] T. Fulghesu,[13] G. Galati,[24,o] M. D. Galati,[38] A. Gallas Torreira,[48] D. Galli,[25,g]
S. Gambetta,[60] M. Gandelman,[3] P. Gandini,[30] B. Ganie,[64] H. Gao,[7] R. Gao,[65] T. Q. Gao,[57] Y. Gao,[8] Y. Gao,[6]
Y. Gao,[8] L. M. Garcia Martin,[51] P. Garcia Moreno,[46] J. García Pardiñas,[66] P. Gardner,[68] L. Garrido,[46]
C. Gaspar,[50] A. Gavrikov,[33] L. L. Gerken,[19] E. Gersabeck,[20] M. Gersabeck,[20] T. Gershon,[58] S. Ghizzo,[29,h]
Z. Ghorbanimoghaddam,[56] F. I. Giasemis,[16,q] V. Gibson,[57] H. K. Giemza,[42] A. L. Gilman,[67] M. Giovannetti,[28]
A. Gioventù,[46] L. Girardey,[64,59] M. A. Giza,[41] F. C. Glaser,[14,22] V. V. Gligorov,[16] C. Göbel,[71]
L. Golinka-Bezshyyko,[87] E. Golobardes,[47] D. Golubkov,[44] A. Golutvin,[63,50] S. Gomez Fernandez,[46]
W. Gomulka,[40] I. Gonçales Vaz,[50] F. Goncalves Abrantes,[65] M. Goncerz,[41] G. Gong,[4,k] J. A. Gooding,[19]
I. V. Gorelov,[44] C. Gotti,[31] E. Govorkova,[66] J. P. Grabowski,[30] L. A. Granado Cardoso,[50] E. Graugés,[46]
E. Graverini,[35,51] L. Grazette,[58] G. Graziani,[27] A. T. Grecu,[43] N. A. Grieser,[67] L. Grillo,[61] S. Gromov,[44]
C. Gu,[15] M. Guarise,[26] L. Guerry,[11] A.-K. Guseinov,[51] E. Gushchin,[44] Y. Guz,[6,50] T. Gys,[50] K. Habermann,[18]
T. Hadavizadeh,[1] C. Hadjivasiliou,[68] G. Haefeli,[51] C. Haen,[50] S. Haken,[57] G. Hallett,[58] P. M. Hamilton,[68]
J. Hammerich,[62] Q. Han,[33] X. Han,[22,50] S. Hansmann-Menzemer,[22] L. Hao,[7] N. Harnew,[65] T. H. Harris,[1]
M. Hartmann,[14] S. Hashmi,[40] J. He,[7,r] N. Heatley,[14] A. Hedes,[64] F. Hemmer,[50] C. Henderson,[67]
R. Henderson,[14] R. D. L. Henderson,[1] A. M. Hennequin,[50] K. Hennessy,[62] L. Henry,[51] J. Herd,[63]
P. Herrero Gascon,[22] J. Heuel,[17] A. Heyn,[13] A. Hicheur,[3] G. Hijano Mendizabal,[52] J. Horswill,[64] R. Hou,[8]
Y. Hou,[11] D. C. Houston,[61] N. Howarth,[62] W. Hu,[7] X. Hu,[4] W. Hulsbergen,[38] R. J. Hunter,[58] M. Hushchyn,[44]
D. Hutchcroft,[62] M. Idzik,[40] D. Ilin,[44] P. Ilten,[67] A. Iniukhin,[44] A. Iohner,[10] A. Ishteev,[44] K. Ivshin,[44]
H. Jage,[17] S. J. Jaimes Elles,[78,49,50] S. Jakobsen,[50] T. Jakoubek,[79] E. Jans,[38] B. K. Jashal,[49] A. Jawahery,[68]
C. Jayaweera,[55] A. Jelavic,[1] V. Jevtic,[19] Z. Jia,[16] E. Jiang,[68] X. Jiang,[5,7] Y. Jiang,[7] Y. J. Jiang,[6]
E. Jimenez Moya,[9] N. Jindal,[89] M. John,[65] A. John Rubesh Rajan,[23] D. Johnson,[55] C. R. Jones,[57] S. Joshi,[42]
B. Jost,[50] J. Juan Castella,[57] N. Jurik,[50] I. Juszczak,[41] K. Kalecinska,[40] D. Kaminaris,[51] S. Kandybei,[53]
M. Kane,[60] Y. Kang,[4,k] C. Kar,[11] M. Karacson,[50] A. Kauniskangas,[51] J. W. Kautz,[67] M. K. Kazanecki,[41]
F. Keizer,[50] M. Kenzie,[57] T. Ketel,[38] B. Khanji,[70] A. Kharisova,[44] S. Kholodenko,[63,50] G. Khreich,[14] F. Kiraz,[14]
T. Kirn,[17] V. S. Kirsebom,[31,b] S. Klaver,[39] N. Kleijne,[35,i] A. Kleimenova,[51] D. K. Klekots,[87] K. Klimaszewski,[42]
M. R. Kmiec,[42] T. Knospe,[19] R. Kolb,[22] S. Koliiev,[54] L. Kolk,[19] A. Konoplyannikov,[6] P. Kopciewicz,[50]
P. Koppenburg,[38] A. Korchin,[53] I. Kostiuk,[38] O. Kot,[54] S. Kotriakhova,[32] E. Kowalczyk,[68] A. Kozachuk,[44]
P. Kravchenko,[44] L. Kravchuk,[44] O. Kravcov,[82] M. Kreps,[58] P. Krokovny,[44] W. Krupa,[70] W. Krzemien,[42]
O. Kshyvanskyi,[54] S. Kubis,[85] M. Kucharczyk,[41] V. Kudryavtsev,[44] E. Kulikova,[44] A. Kupsc,[86] V. Kushnir,[53]

B. Kutsenko,[13] J. Kvapil,[69] I. Kyryllin,[53] D. Lacarrere,[50] P. Laguarta Gonzalez,[46] A. Lai,[32] Y. Lai,[73] A. Lampis,[32] D. Lancierini,[63] C. Landesa Gomez,[48] J. J. Lane,[1] G. Lanfranchi,[28] C. Langenbruch,[22] J. Langer,[19] T. Latham,[58] F. Lazzari,[35,s] C. Lazzeroni,[55] R. Le Gac,[13] H. Lee,[62] R. Lefèvre,[11] A. Leflat,[44] S. Legotin,[44] M. Lehuraux,[58] E. Lemos Cid,[50] O. Leroy,[13] T. Lesiak,[41] E. D. Lesser,[50] B. Leverington,[22] A. Li,[4,k] C. Li,[4,k] C. Li,[13] H. Li,[74] J. Li,[8] K. Li,[77] L. Li,[64] M. Li,[8] P. Li,[7] P.-R. Li,[75] Q. Li,[5,7] T. Li,[73] T. Li,[74] Y. Li,[8] Y. Li,[5] Y. Li,[4] Z. Lian,[4,k] Q. Liang,[8] X. Liang,[70] Z. Liang,[32] S. Libralon,[49] A. Lightbody,[12] C. Lin,[7] T. Lin,[59] R. Lindner,[50] H. Linton,[63] R. Litvinov,[32] D. Liu,[8] F. L. Liu,[1] G. Liu,[74] K. Liu,[75] S. Liu,[5] W. Liu,[8] Y. Liu,[60] Y. Liu,[75] Y. L. Liu,[63] G. Loachamin Ordonez,[71] I. Lobo,[1] A. Lobo Salvia,[46] A. Loi,[32] T. Long,[57] F. C. L. Lopes,[2,f] J. H. Lopes,[3] A. Lopez Huertas,[46] C. Lopez Iribarnegaray,[48] S. López Soliño,[48] Q. Lu,[15] C. Lucarelli,[50] D. Lucchesi,[33,t] M. Lucio Martinez,[49] Y. Luo,[6] A. Lupato,[33,u] E. Luppi,[26,e] K. Lynch,[23] X.-R. Lyu,[7] G. M. Ma,[4,k] H. Ma,[73] S. Maccolini,[19] F. Machefert,[14] F. Maciuc,[43] B. Mack,[70] I. Mackay,[65] L. M. Mackey,[70] L. R. Madhan Mohan,[57] M. J. Madurai,[55] D. Magdalinski,[38] D. Maisuzenko,[44] J. J. Malczewski,[41] S. Malde,[65] L. Malentacca,[50] A. Malinin,[44] T. Maltsev,[44] G. Manca,[32,m] G. Mancinelli,[13] C. Mancuso,[14] R. Manera Escalero,[46] F. M. Manganella,[37] D. Manuzzi,[25] D. Marangotto,[30,j] J. F. Marchand,[10] R. Marchevski,[51] U. Marconi,[25] E. Mariani,[16] S. Mariani,[50] C. Marin Benito,[46] J. Marks,[22] A. M. Marshall,[56] L. Martel,[65] G. Martelli,[34] G. Martellotti,[36] L. Martinazzoli,[50] M. Martinelli,[31,b] D. Martinez Gomez,[83] D. Martinez Santos,[45] F. Martinez Vidal,[49] A. Martorell i Granollers,[47] A. Massafferri,[2] R. Matev,[50] A. Mathad,[50] V. Matiunin,[44] C. Matteuzzi,[70] K. R. Mattioli,[15] A. Mauri,[63] E. Maurice,[15] J. Mauricio,[46] P. Mayencourt,[51] J. Mazorra de Cos,[49] M. Mazurek,[42] D. Mazzanti Tarancon,[46] M. McCann,[63] N. T. McHugh,[61] A. McNab,[64] R. McNulty,[23] B. Meadows,[67] D. Melnychuk,[42] D. Mendoza Granada,[16] P. Menendez Valdes Perez,[48] F. M. Meng,[4,k] M. Merk,[38,84] A. Merli,[51,30] L. Meyer Garcia,[68] D. Miao,[5,7] H. Miao,[7] M. Mikhasenko,[80] D. A. Milanes,[78,v] A. Minotti,[31,b] E. Minucci,[28] T. Miralles,[11] B. Mitreska,[64] D. S. Mitzel,[19] R. Mocanu,[43] A. Modak,[59] L. Moeser,[19] R. D. Moise,[17] E. F. Molina Cardenas,[88] T. Mombächer,[67] M. Monk,[57] T. Monnard,[51] S. Monteil,[11] A. Morcillo Gomez,[48] G. Morello,[28] M. J. Morello,[35,i] M. P. Morgenthaler,[22] A. Moro,[31,b] J. Moron,[40] W. Morren,[38] A. B. Morris,[82,50] A. G. Morris,[13] R. Mountain,[70] Z. M. Mu,[6] E. Muhammad,[58] F. Muheim,[60] M. Mulder,[38] K. Müller,[52] F. Muñoz-Rojas,[9] R. Murta,[63] V. Mytrochenko,[53] P. Naik,[62] T. Nakada,[51] R. Nandakumar,[59] T. Nanut,[50] G. Napoletano,[51] I. Nasteva,[3] M. Needham,[60] E. Nekrasova,[44] N. Neri,[30,j] S. Neubert,[18] N. Neufeld,[50] P. Neustroev,[44] J. Nicolini,[50] D. Nicotra,[84] E. M. Niel,[15] N. Nikitin,[44] L. Nisi,[19] Q. Niu,[75] B. K. Njoki,[50] P. Nogarolli,[3] P. Nogga,[18] C. Normand,[48] J. Novoa Fernandez,[48] G. Nowak,[67] C. Nunez,[88] H. N. Nur,[61] A. Oblakowska-Mucha,[40] V. Obraztsov,[44] T. Oeser,[17] A. Okhotnikov,[44] O. Okhrimenko,[54] R. Oldeman,[32,m] F. Oliva,[60,50] E. Olivart Pino,[46] M. Olocco,[19] R. H. O'Neil,[50] J. S. Ordonez Soto,[11] D. Osthues,[19] J. M. Otalora Goicochea,[3] P. Owen,[52] A. Oyanguren,[49] O. Ozcelik,[50] F. Paciolla,[35,w] A. Padee,[42] K. O. Padeken,[18] B. Pagare,[48] T. Pajero,[50] A. Palano,[24] L. Palini,[30] M. Palutan,[28] C. Pan,[76] X. Pan,[4,k] S. Panebianco,[12] S. Paniskaki,[50,33] G. Panshin,[5] L. Paolucci,[64] A. Papanestis,[59] M. Pappagallo,[24,o] L. L. Pappalardo,[26] C. Pappenheimer,[67] C. Parkes,[64] D. Parmar,[80] G. Passaleva,[27] D. Passaro,[35,i] A. Pastore,[24] M. Patel,[63] J. Patoc,[65] C. Patrignani,[25,g] A. Paul,[70] C. J. Pawley,[84] A. Pellegrino,[38] J. Peng,[5,7] X. Peng,[75] M. Pepe Altarelli,[28] S. Perazzini,[25] D. Pereima,[44] H. Pereira Da Costa,[69] M. Pereira Martinez,[48] A. Pereiro Castro,[48] C. Perez,[47] P. Perret,[11] A. Perrevoort,[83] A. Perro,[74] M. J. Peters,[67] K. Petridis,[56] A. Petrolini,[29,h] S. Pezzulo,[29,h] J. P. Pfaller,[67] H. Pham,[70] L. Pica,[35,i] M. Piccini,[34] L. Piccolo,[32] B. Pietrzyk,[10] G. Pietrzyk,[14] R. N. Pilato,[62] D. Pinci,[36] F. Pisani,[50] M. Pizzichemi,[31,50,b] V. M. Placinta,[43] M. Plo Casasus,[48] T. Poeschl,[50] F. Polci,[16] M. Poli Lener,[28] A. Poluektov,[13] N. Polukhina,[44] I. Polyakov,[64] E. Polycarpo,[3] S. Ponce,[50] D. Popov,[7,50] K. Popp,[19] S. Poslavskii,[44] K. Prasanth,[60] C. Prouve,[45] D. Provenzano,[32,50,m] V. Pugatch,[54] A. Puicercus Gomez,[50] G. Punzi,[35,s] J. R. Pybus,[69] Q. Q. Qian,[6] W. Qian,[7] N. Qin,[4,k] R. Quagliani,[50] R. I. Rabadan Trejo,[58] R. Racz,[82] J. H. Rademacker,[56] M. Rama,[35] M. Ramírez García,[88] V. Ramos De Oliveira,[71] M. Ramos Pernas,[58] M. S. Rangel,[3] F. Ratnikov,[44] G. Raven,[39] M. Rebollo De Miguel,[49] F. Redi,[30,u] J. Reich,[56] F. Reiss,[20] Z. Ren,[7] P. K. Resmi,[65] M. Ribalda Galvez,[46] R. Ribatti,[51] G. Ricart,[12] D. Riccardi,[35,i] S. Ricciardi,[59] K. Richardson,[66] M. Richardson-Slipper,[57] F. Riehn,[19] K. Rinnert,[62] P. Robbe,[14,50] G. Robertson,[61] E. Rodrigues,[62] A. Rodriguez Alvarez,[46] E. Rodriguez Fernandez,[48] J. A. Rodriguez Lopez,[78] E. Rodriguez Rodriguez,[50] J. Roensch,[19] A. Rogachev,[44] A. Rogovskiy,[59] D. L. Rolf,[19]

P. Roloff,[50] V. Romanovskiy,[67] A. Romero Vidal,[48] G. Romolini,[26,50] F. Ronchetti,[51] T. Rong,[6] M. Rotondo,[28]
S. R. Roy,[22] M. S. Rudolph,[70] M. Ruiz Diaz,[22] R. A. Ruiz Fernandez,[48] J. Ruiz Vidal,[84] J. J. Saavedra-Arias,[9]
J. J. Saborido Silva,[48] S. E. R. Sacha Emile R.,[50] N. Sagidova,[44] D. Sahoo,[81] N. Sahoo,[55] B. Saitta,[32]
M. Salomoni,[31,50,b] I. Sanderswood,[49] R. Santacesaria,[36] C. Santamarina Rios,[48] M. Santimaria,[28] L. Santoro,[2]
E. Santovetti,[37] A. Saputi,[26,50] D. Saranin,[44] A. Sarnatskiy,[83] G. Sarpis,[50] M. Sarpis,[82] C. Satriano,[36]
A. Satta,[37] M. Saur,[75] D. Savrina,[44] H. Sazak,[17] F. Sborzacchi,[50,28] A. Scarabotto,[19] S. Schael,[17] S. Scherl,[62]
M. Schiller,[22] H. Schindler,[50] M. Schmelling,[21] B. Schmidt,[50] N. Schmidt,[69] S. Schmitt,[66] H. Schmitz,[18]
O. Schneider,[51] A. Schopper,[63] N. Schulte,[19] M. H. Schune,[14] G. Schwering,[17] B. Sciascia,[28] A. Sciuccati,[50]
G. Scriven,[84] I. Segal,[80] S. Sellam,[48] A. Semennikov,[44] T. Senger,[52] M. Senghi Soares,[39] A. Sergi,[29,h]
N. Serra,[52] L. Sestini,[27] A. Seuthe,[19] B. Sevilla Sanjuan,[47] Y. Shang,[6] D. M. Shangase,[88] M. Shapkin,[44]
R. S. Sharma,[70] I. Shchemerov,[44] L. Shchutska,[51] T. Shears,[62] L. Shekhtman,[44] Z. Shen,[38] S. Sheng,[51]
V. Shevchenko,[44] B. Shi,[7] J. Shi,[57] Q. Shi,[7] W. S. Shi,[74] Y. Shimizu,[14] E. Shmanin,[25] R. Shorkin,[44]
J. D. Shupperd,[70] R. Silva Coutinho,[2] G. Simi,[33,t] S. Simone,[24,o] M. Singha,[81] I. Siral,[51] N. Skidmore,[58]
T. Skwarnicki,[70] M. W. Slater,[55] E. Smith,[66] M. Smith,[63] L. Soares Lavra,[60] M. D. Sokoloff,[67] F. J. P. Soler,[61]
A. Solomin,[56] A. Solovev,[44] K. Solovieva,[20] N. S. Sommerfeld,[18] R. Song,[1] Y. Song,[51] Y. Song,[4,k]
Y. S. Song,[6] F. L. Souza De Almeida,[46] B. Souza De Paula,[3] K. M. Sowa,[40] E. Spadaro Norella,[29,h]
E. Spedicato,[25] J. G. Speer,[19] P. Spradlin,[61] F. Stagni,[50] M. Stahl,[80] S. Stahl,[50] S. Stanislaus,[65] M. Stefaniak,[89]
O. Steinkamp,[52] D. Strekalina,[44] Y. Su,[7] F. Suljik,[65] J. Sun,[32] J. Sun,[64] L. Sun,[76] D. Sundfeld,[2]
W. Sutcliffe,[52] P. Svihra,[79] V. Svintozelskyi,[49] K. Swientek,[40] F. Swystun,[57] A. Szabelski,[42] T. Szumlak,[40]
Y. Tan,[4] Y. Tang,[76] Y. T. Tang,[7] M. D. Tat,[22] J. A. Teijeiro Jimenez,[48] A. Terentev,[44] F. Terzuoli,[35,w]
F. Teubert,[50] E. Thomas,[50] D. J. D. Thompson,[55] A. R. Thomson-Strong,[60] H. Tilquin,[63] V. Tisserand,[11]
S. T'Jampens,[10] M. Tobin,[5,50] T. T. Todorov,[20] L. Tomassetti,[26,e] G. Tonani,[30] X. Tong,[6] T. Tork,[30]
L. Toscano,[19] D. Y. Tou,[4,k] C. Trippl,[47] G. Tuci,[22] N. Tuning,[38] L. H. Uecker,[22] A. Ukleja,[40] D. J. Unverzagt,[22]
A. Upadhyay,[50] B. Urbach,[60] A. Usachov,[38] A. Ustyuzhanin,[44] U. Uwer,[22] V. Vagnoni,[25,50] A. Vaitkevicius,[82]
V. Valcarce Cadenas,[48] G. Valenti,[25] N. Valls Canudas,[50] J. van Eldik,[50] H. Van Hecke,[69] E. van Herwijnen,[63]
C. B. Van Hulse,[48,x] R. Van Laak,[51] M. van Veghel,[84] G. Vasquez,[52] R. Vazquez Gomez,[46] P. Vazquez Regueiro,[48]
C. Vázquez Sierra,[45] S. Vecchi,[26] J. Velilla Serna,[49] J. J. Velthuis,[56] M. Veltri,[27,y] A. Venkateswaran,[51]
M. Verdoglia,[32] M. Vesterinen,[58] W. Vetens,[70] D. Vico Benet,[65] P. Vidrier Villalba,[46] M. Vieites Diaz,[48]
X. Vilasis-Cardona,[47] E. Vilella Figueras,[62] A. Villa,[25] P. Vincent,[16] B. Vivacqua,[3] F. C. Volle,[55]
D. vom Bruch,[13] N. Voropaev,[44] K. Vos,[84] C. Vrahas,[60] J. Wagner,[19] J. Walsh,[35] E. J. Walton,[1] G. Wan,[6]
A. Wang,[7] B. Wang,[5] C. Wang,[22] G. Wang,[8] H. Wang,[75] J. Wang,[7] J. Wang,[5] J. Wang,[4,k] J. Wang,[76]
L. Wang,[73] M. Wang,[50] N. W. Wang,[7] R. Wang,[56] X. Wang,[8] X. Wang,[74] X. W. Wang,[63] Y. Wang,[77]
Y. Wang,[6] Y. H. Wang,[75] Z. Wang,[14] Z. Wang,[30] J. A. Ward,[58,1] M. Waterlaat,[50] N. K. Watson,[55]
D. Websdale,[63] Y. Wei,[6] Z. Weida,[7] J. Wendel,[45] B. D. C. Westhenry,[56] C. White,[57] M. Whitehead,[61]
E. Whiter,[55] A. R. Wiederhold,[64] D. Wiedner,[19] M. A. Wiegertjes,[38] C. Wild,[65] G. Wilkinson,[65,50]
M. K. Wilkinson,[67] M. Williams,[66] M. J. Williams,[50] M. R. J. Williams,[60] R. Williams,[57] S. Williams,[56]
Z. Williams,[56] F. F. Wilson,[59] M. Winn,[12] W. Wislicki,[42] M. Witek,[41] L. Witola,[19] T. Wolf,[22] E. Wood,[57]
G. Wormser,[14] S. A. Wotton,[57] H. Wu,[70] J. Wu,[8] X. Wu,[76] Y. Wu,[6,57] Z. Wu,[7] K. Wyllie,[50] S. Xian,[74]
Z. Xiang,[5] Y. Xie,[8] T. X. Xing,[30] A. Xu,[35,i] L. Xu,[4,k] M. Xu,[50] Z. Xu,[50] Z. Xu,[7] Z. Xu,[5] S. Yadav,[26]
K. Yang,[63] X. Yang,[6] Y. Yang,[7] Y. Yang,[81] Z. Yang,[6] V. Yeroshenko,[14] H. Yeung,[64] H. Yin,[8] X. Yin,[7]
C. Y. Yu,[6] J. Yu,[73] X. Yuan,[5] Y Yuan,[5,7] J. A. Zamora Saa,[72] M. Zavertyaev,[21] M. Zdybal,[41] F. Zenesini,[25]
C. Zeng,[5,7] M. Zeng,[4,k] C. Zhang,[6] D. Zhang,[8] J. Zhang,[7] L. Zhang,[4,k] R. Zhang,[8] S. Zhang,[65] S. L. Zhang,[73]
Y. Zhang,[6] Y. Z. Zhang,[4,k] Z. Zhang,[4,k] Y. Zhao,[22] A. Zhelezov,[22] S. Z. Zheng,[6] X. Z. Zheng,[4,k] Y. Zheng,[7]
T. Zhou,[6] X. Zhou,[8] Y. Zhou,[7] V. Zhovkovska,[58] L. Z. Zhu,[7] X. Zhu,[4,k] X. Zhu,[8] Y. Zhu,[17] V. Zhukov,[17]
J. Zhuo,[49] D. Zuliani,[33,t] and G. Zunica[28]

(LHCb Collaboration)

[1]*School of Physics and Astronomy, Monash University, Melbourne, Australia*
[2]*Centro Brasileiro de Pesquisas Físicas (CBPF), Rio de Janeiro, Brazil*
[3]*Universidade Federal do Rio de Janeiro (UFRJ), Rio de Janeiro, Brazil*
[4]*Department of Engineering Physics, Tsinghua University, Beijing, China*
[5]*Institute of High Energy Physics (IHEP), Beijing, China*
[6]*School of Physics State Key Laboratory of Nuclear Physics and Technology, Peking University, Beijing, China*
[7]*University of Chinese Academy of Sciences, Beijing, China*
[8]*Institute of Particle Physics, Central China Normal University, Wuhan, Hubei, China*
[9]*Consejo Nacional de Rectores (CONARE), San Jose, Costa Rica*
[10]*Université Savoie Mont Blanc, CNRS, IN2P3-LAPP, Annecy, France*
[11]*Université Clermont Auvergne, CNRS/IN2P3, LPC, Clermont-Ferrand, France*
[12]*Université Paris-Saclay, Centre d'Etudes de Saclay (CEA), IRFU, Gif-Sur-Yvette, France*
[13]*Aix-Marseille University, CNRS/IN2P3, CPPM, Marseille, France*
[14]*Université Paris-Saclay, CNRS/IN2P3, IJCLab, Orsay, France*
[15]*Laboratoire Leprince-Ringuet, CNRS/IN2P3, Ecole Polytechnique, Institut Polytechnique de Paris, Palaiseau, France*
[16]*Laboratoire de Physique Nucléaire et de Hautes Énergies (LPNHE), Sorbonne Université, CNRS/IN2P3, Paris, France*
[17]*I. Physikalisches Institut, RWTH Aachen University, Aachen, Germany*
[18]*Universität Bonn—Helmholtz-Institut für Strahlen und Kernphysik, Bonn, Germany*
[19]*Fakultät Physik, Technische Universität Dortmund, Dortmund, Germany*
[20]*Physikalisches Institut, Albert-Ludwigs-Universität Freiburg, Freiburg, Germany*
[21]*Max-Planck-Institut für Kernphysik (MPIK), Heidelberg, Germany*
[22]*Physikalisches Institut, Ruprecht-Karls-Universität Heidelberg, Heidelberg, Germany*
[23]*School of Physics, University College Dublin, Dublin, Ireland*
[24]*INFN Sezione di Bari, Bari, Italy*
[25]*INFN Sezione di Bologna, Bologna, Italy*
[26]*INFN Sezione di Ferrara, Ferrara, Italy*
[27]*INFN Sezione di Firenze, Firenze, Italy*
[28]*INFN Laboratori Nazionali di Frascati, Frascati, Italy*
[29]*INFN Sezione di Genova, Genova, Italy*
[30]*INFN Sezione di Milano, Milano, Italy*
[31]*INFN Sezione di Milano-Bicocca, Milano, Italy*
[32]*INFN Sezione di Cagliari, Monserrato, Italy*
[33]*INFN Sezione di Padova, Padova, Italy*
[34]*INFN Sezione di Perugia, Perugia, Italy*
[35]*INFN Sezione di Pisa, Pisa, Italy*
[36]*INFN Sezione di Roma La Sapienza, Roma, Italy*
[37]*INFN Sezione di Roma Tor Vergata, Roma, Italy*
[38]*Nikhef National Institute for Subatomic Physics, Amsterdam, Netherlands*
[39]*Nikhef National Institute for Subatomic Physics and VU University Amsterdam, Amsterdam, Netherlands*
[40]*AGH—University of Krakow, Faculty of Physics and Applied Computer Science, Kraków, Poland*
[41]*Henryk Niewodniczanski Institute of Nuclear Physics Polish Academy of Sciences, Kraków, Poland*
[42]*National Center for Nuclear Research (NCBJ), Warsaw, Poland*
[43]*Horia Hulubei National Institute of Physics and Nuclear Engineering, Bucharest-Magurele, Romania*
[44]*Authors affiliated with an institute formerly covered by a cooperation agreement with CERN*
[45]*Universidade da Coruña, A Coruña, Spain*
[46]*ICCUB, Universitat de Barcelona, Barcelona, Spain*
[47]*La Salle, Universitat Ramon Llull, Barcelona, Spain*
[48]*Instituto Galego de Física de Altas Enerxías (IGFAE), Universidade de Santiago de Compostela, Santiago de Compostela, Spain*
[49]*Instituto de Fisica Corpuscular, Centro Mixto Universidad de Valencia—CSIC, Valencia, Spain*
[50]*European Organization for Nuclear Research (CERN), Geneva, Switzerland*
[51]*Institute of Physics, Ecole Polytechnique Fédérale de Lausanne (EPFL), Lausanne, Switzerland*
[52]*Physik-Institut, Universität Zürich, Zürich, Switzerland*
[53]*NSC Kharkiv Institute of Physics and Technology (NSC KIPT), Kharkiv, Ukraine*
[54]*Institute for Nuclear Research of the National Academy of Sciences (KINR), Kyiv, Ukraine*
[55]*School of Physics and Astronomy, University of Birmingham, Birmingham, United Kingdom*
[56]*H.H. Wills Physics Laboratory, University of Bristol, Bristol, United Kingdom*
[57]*Cavendish Laboratory, University of Cambridge, Cambridge, United Kingdom*
[58]*Department of Physics, University of Warwick, Coventry, United Kingdom*
[59]*STFC Rutherford Appleton Laboratory, Didcot, United Kingdom*
[60]*School of Physics and Astronomy, University of Edinburgh, Edinburgh, United Kingdom*

[61]*School of Physics and Astronomy, University of Glasgow, Glasgow, United Kingdom*
[62]*Oliver Lodge Laboratory, University of Liverpool, Liverpool, United Kingdom*
[63]*Imperial College London, London, United Kingdom*
[64]*Department of Physics and Astronomy, University of Manchester, Manchester, United Kingdom*
[65]*Department of Physics, University of Oxford, Oxford, United Kingdom*
[66]*Massachusetts Institute of Technology, Cambridge, Massachusetts, USA*
[67]*University of Cincinnati, Cincinnati, Ohio, USA*
[68]*University of Maryland, College Park, Maryland, USA*
[69]*Los Alamos National Laboratory (LANL), Los Alamos, New Mexico, USA*
[70]*Syracuse University, Syracuse, New York, USA*
[71]*Pontifícia Universidade Católica do Rio de Janeiro (PUC-Rio), Rio de Janeiro, Brazil*
(associated with Universidade Federal do Rio de Janeiro (UFRJ), Rio de Janeiro, Brazil)
[72]*Universidad Andres Bello, Santiago, Chile*
(associated with Physik-Institut, Universität Zürich, Zürich, Switzerland)
[73]*School of Physics and Electronics, Hunan University, Changsha City, China*
(associated with Institute of Particle Physics, Central China Normal University, Wuhan, Hubei, China)
[74]*State Key Laboratory of Nuclear Physics and Technology, South China Normal University, Guangzhou, China*
(associated with Department of Engineering Physics, Tsinghua University, Beijing, China)
[75]*Lanzhou University, Lanzhou, China*
(associated with Institute of High Energy Physics (IHEP), Beijing, China)
[76]*School of Physics and Technology, Wuhan University, Wuhan, China*
(associated with Department of Engineering Physics, Tsinghua University, Beijing, China)
[77]*Henan Normal University, Xinxiang, China*
(associated with Institute of Particle Physics, Central China Normal University, Wuhan, Hubei, China)
[78]*Departamento de Fisica, Universidad Nacional de Colombia, Bogota, Colombia*
(associated with Laboratoire de Physique Nucléaire et de Hautes Énergies (LPNHE),
Sorbonne Université, CNRS/IN2P3, Paris, France)
[79]*Institute of Physics of the Czech Academy of Sciences, Prague, Czech Republic*
(associated with Department of Physics and Astronomy, University of Manchester, Manchester, United Kingdom)
[80]*Ruhr Universitaet Bochum, Fakultaet f. Physik und Astronomie, Bochum, Germany*
(associated with Fakultät Physik, Technische Universität Dortmund, Dortmund, Germany)
[81]*Eotvos Lorand University, Budapest, Hungary*
(associated with European Organization for Nuclear Research (CERN), Geneva, Switzerland)
[82]*Faculty of Physics, Vilnius University, Vilnius, Lithuania*
(associated with Physikalisches Institut, Albert-Ludwigs-Universität Freiburg, Freiburg, Germany)
[83]*Van Swinderen Institute, University of Groningen, Groningen, Netherlands*
(associated with Nikhef National Institute for Subatomic Physics, Amsterdam, Netherlands)
[84]*Universiteit Maastricht, Maastricht, Netherlands*
(associated with Nikhef National Institute for Subatomic Physics, Amsterdam, Netherlands)
[85]*Tadeusz Kosciuszko Cracow University of Technology, Cracow, Poland*
(associated with Henryk Niewodniczanski Institute of Nuclear Physics Polish Academy of Sciences, Kraków, Poland)
[86]*Department of Physics and Astronomy, Uppsala University, Uppsala, Sweden*
(associated with School of Physics and Astronomy, University of Glasgow, Glasgow, United Kingdom)
[87]*Taras Schevchenko University of Kyiv, Faculty of Physics, Kyiv, Ukraine*
(associated with Université Paris-Saclay, CNRS/IN2P3, IJCLab, Orsay, France)
[88]*University of Michigan, Ann Arbor, Michigan, USA*
(associated with Syracuse University, Syracuse, New York, USA)
[89]*Ohio State University, Columbus, Ohio, USA*
(associated with Los Alamos National Laboratory (LANL), Los Alamos, New Mexico, USA)

[a] Also at Lamarr Institute for Machine Learning and Artificial Intelligence, Dortmund, Germany.
[b] Also at Università degli Studi di Milano-Bicocca, Milano, Italy.
[c] Also at Università di Modena e Reggio Emilia, Modena, Italy.
[d] Also at Department of Physics and Astronomy, University of Victoria, Victoria, Canada.
[e] Also at Università di Ferrara, Ferrara, Italy.
[f] Also at Universidade Estadual de Campinas (UNICAMP), Campinas, Brazil.
[g] Also at Università di Bologna, Bologna, Italy.
[h] Also at Università di Genova, Genova, Italy.
[i] Also at Scuola Normale Superiore, Pisa, Italy.
[j] Also at Università degli Studi di Milano, Milano, Italy.

[k]Also at Center for High Energy Physics, Tsinghua University, Beijing, China.
[l]Also at Universidad Nacional Autónoma de Honduras, Tegucigalpa, Honduras.
[m]Also at Università di Cagliari, Cagliari, Italy.
[n]Also at Centro Federal de Educacão Tecnológica Celso Suckow da Fonseca, Rio De Janeiro, Brazil.
[o]Also at Università di Bari, Bari, Italy.
[p]Also at Università di Perugia, Perugia, Italy.
[q]Also at LIP6, Sorbonne Université, Paris, France.
[r]Also at Hangzhou Institute for Advanced Study, UCAS, Hangzhou, China.
[s]Also at Università di Pisa, Pisa, Italy.
[t]Also at Università di Padova, Padova, Italy.
[u]Also at Università di Bergamo, Bergamo, Italy.
[v]Also at Universidad de Ingeniería y Tecnología (UTEC), Lima, Peru.
[w]Also at Università di Siena, Siena, Italy.
[x]Also at Universidad de Alcalá, Alcalá de Henares, Spain.
[y]Also at Università di Urbino, Urbino, Italy.